

SCIENTIFIC REPORTS



OPEN

Negative differential resistance and bias-modulated metal-to-insulator transition in zigzag C_2N - $h2D$ nanoribbon

Received: 18 May 2016
Accepted: 01 February 2017
Published: 06 April 2017

Jing-Jing He^{1,2}, Yan-Dong Guo^{1,2} & Xiao-Hong Yan^{1,2,3}

Motivated by the fabrication of layered two-dimensional material C_2N - $h2D$ [*Nat. Commun.* **6**, 6486 (2015)], we cut the single-layer C_2N - $h2D$ into a zigzag nanoribbon and perform a theoretical study. The results indicate that the band structure changes from semiconducting to metallic and a negative differential resistance effect occurs in the I - V curve. Interestingly, the current can be reduced to zero and this insulator-like state can be maintained as the bias increases. We find this unique property is originated from a peculiar band morphology, with only two subbands appearing around the Fermi level while others being far away. Furthermore the width and symmetry of the zigzag C_2N - $h2D$ nanoribbon can be used to tune the transport properties, such as cut-off bias and the maximum current. We also explore the electron transport property of an aperiodic model composed of two nanoribbons with different widths and obtain the same conclusion. This mechanism can be extended to other systems, e.g., hybrid BCN nanoribbons. Our discoveries suggest that the zigzag C_2N - $h2D$ nanoribbon has great potential in nanoelectronics applications.

Two-dimensional (2D) materials have attracted tremendous attention for applications in future nanoelectronics owing to their physical, electrical and chemical properties¹. As a typical 2D material, graphene exhibits high strength, extraordinary conductivity and excellent transmittance^{2,3}. However, the absence of a band gap limits its application in nanoelectronics and optoelectronics^{4–7}. Recently, a novel 2D layered material C_2N - $h2D$ has been synthesized via a simple wet-chemical reaction^{8,9}. The C_2N - $h2D$ material possesses evenly distributed nitrogen atoms and holes. Compared to graphene, its band opens a direct gap of 1.70 eV, and the field-effect-transistor fabricated thereon has a high on/off ratio of 10^7 , suggesting great potential in device application. In previous studies on fullerenes, carbon nanotubes and graphene-based structures, researchers have found the negative differential resistance (NDR) effect which can be applied to logic operators, molecular switch, memory, oscillator, etc refs 10–14. For example, Ren *et al.*¹⁴ have reported NDR occurs in a doped armchair graphene nanoribbon-based junction, such NDR behavior derives from the interaction between the narrow density of states of the doped leads and the discrete states in the scattering region. Do *et al.*¹⁵ have found the NDR effect may be severely affected by the roughness of ribbon edges in a p^+/p junction based on zigzag-edged graphene. Khoo *et al.*¹⁶ have observed NDR phenomenon in carbon chain-nanotube junctions and find that it is caused by an energy misalignment in even-chain model, however it is produced by the asymmetric distortions of the conducting resonances in odd-chain model. In these theoretical work, all structures are molecular junctions. In this paper, we present a periodic nanoribbon (zigzag C_2N - $h2D$)-based model, and investigate the effect of width and symmetry on its electronic and transport properties. By performing first-principles calculations, we find C_2N - $h2D$ changes from semiconducting to metallic after been cut into a nanoribbon. In order to explore the physical mechanism, we first set up a periodic model. A NDR effect appears in this periodic system, surprisingly, the current can reduce to zero and then this state can be maintained as the bias increases. In a few nano-sized systems, this kind of phenomenon is rarely reported. In-depth study shows that this unique phenomenon stems from the peculiar

¹College of Electronic Science and Engineering, Nanjing University of Posts and Telecommunications, Nanjing 210046, China. ²Key Laboratory of Radio Frequency and Micro-Nano Electronics of Jiangsu Province, Nanjing 210023, Jiangsu, China. ³College of Science, Nanjing University of Aeronautics and Astronautics, Nanjing 210016, China. Correspondence and requests for materials should be addressed to Y.-D.G. (email: yandongguo@njupt.edu.cn) or X.-H.Y. (email: yanxh@njupt.edu.cn)

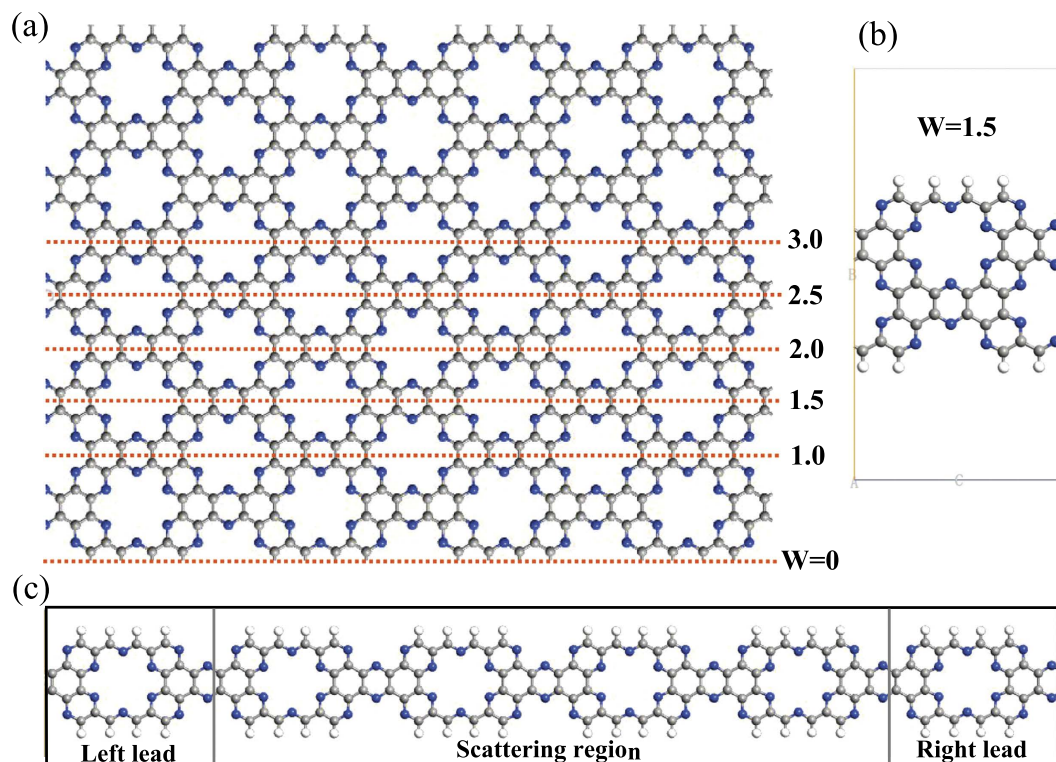


Figure 1. Schematic illustration of (a) Zigzag C₂N-h₂D structures with different widths ($W = 1.0, 1.5, 2.0, 2.5$ and 3.0); (b) The unit cell of $W = 1.5$ models. (c) The two-probe system of zigzag C₂N-h₂D nanoribbon ($W = 1.0$). Nitrogen, carbon and hydrogen atoms are shown by blue, gray and white balls, respectively.

band morphology where there are only two subbands near the Fermi level and others are far away. In addition, the width and symmetry of the zigzag C₂N-h₂D nanoribbon can tune the cut-off bias and the maximum current. We also show that similar electron transport occurs in a heterogeneous model and other materials. These transport properties are quite useful for future nanoelectronic device applications.

Results

Compared to graphene, there are more ways to cut the single-layer C₂N-h₂D into a zigzag nanoribbon due to the presence of holes and nitrogen atoms. Classification can be carried out according to the atomic species of nanoribbon edges, e.g., carbon and nitrogen-edged or carbon-edged. In our research, we select the structure whose edge atoms are all carbon atoms. To show the nanoribbons more intuitively and clearly, here we use W to denote the width and choose $W = 1.0$ to 3.0 models to study. The schematic illustration of zigzag C₂N-h₂D nanoribbons with different widths is shown in Fig. 1(a). The unit cell of $W = 1.5$ model is chosen to be shown in Fig. 1(b). Obviously, when W is an integer ($W = 1.0, 2.0$ and 3.0), the structure is symmetric. If the W is a non-integer ($W = 1.5$ and 2.5), the structure has no symmetry. The two-probe configuration could be divided into three parts, the left semi-infinite zigzag C₂N-h₂D nanoribbon electrode, the central scattering region and the right semi-finite zigzag C₂N-h₂D nanoribbon electrode (as shown in Fig. 1(c)), the length of the central scattering region is 59 \AA which is enough to avoid direct coupling between left and right electrodes¹⁷.

Figure 2(a) presents the current-voltage (I - V) characteristic of the two-probe system with $W = 1.0$. Apparently, a NDR peak appears in our model. The current firstly increases as the bias increases and reaches the maximum when the bias is 0.2 V and then smoothly decreases to zero as the bias increases to 0.5 V . We define 0.5 V as the cut-off bias. Interestingly, as the bias continues to increase, the current maintains at zero. It indicates that the system is in an insulator-like state. This is contrary to its metallic state under a low bias. As far as we know, this phenomenon has not been reported in periodic systems with widths of several nanometers. A similar I - V characteristic can be seen in $W = 1.5$ model as shown in Fig. 2(b), but the cut-off bias and the maximum current decrease due to the increased width.

In order to investigate the physical mechanism of the peculiar I - V characteristic of our models, we first calculate the transmission spectra of $W = 1.5$ model under different biases as shown in Fig. 3. It can be found that as the bias increases the intensity of the transmission peak around the Fermi energy gradually decreases. Owing to the increasing integration region, the current firstly increases under a low bias. When the bias is higher than 0.1 V , the current begins to drop, so a NDR effect occurs. When the bias continues to increase to 0.25 V , the current decreases to zero due to the disappeared transmission peak. It is quite interesting that the insulator-like state can be maintained until the bias increases to 1.0 V .

Figure 4(a) shows the band structure of the unit cell of the $W = 1.5$ zigzag C₂N-h₂D nanoribbon. For better illustration, we define the following variables, $E_{AD} = E_A - E_D$, $E_{AB} = E_A - E_B$ and $E_{CD} = E_C - E_D$ where E_A , E_B , E_C

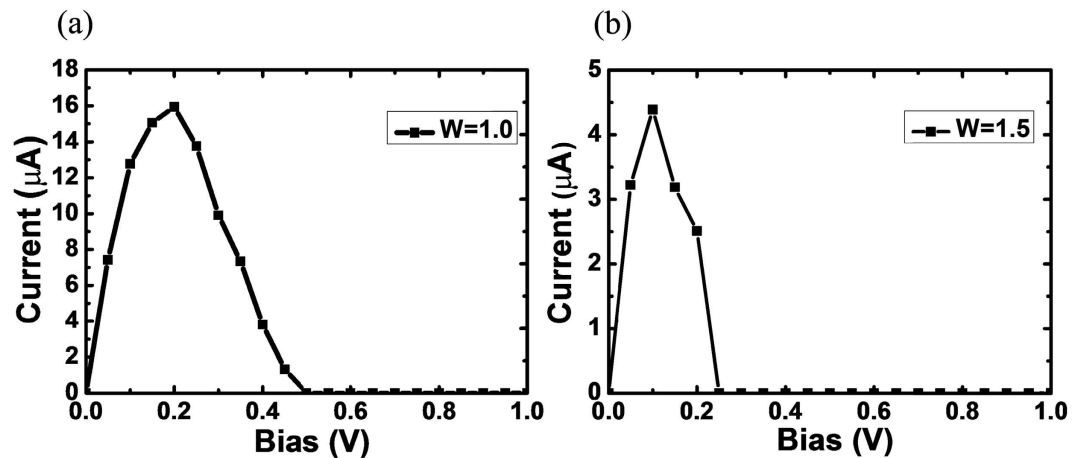


Figure 2. The current-voltage curve of zigzag C_2N - $h2D$ nanoribbon in the bias range from 0.0 to 1.0 V. (a) $W = 1.0$; (b) $W = 1.5$.

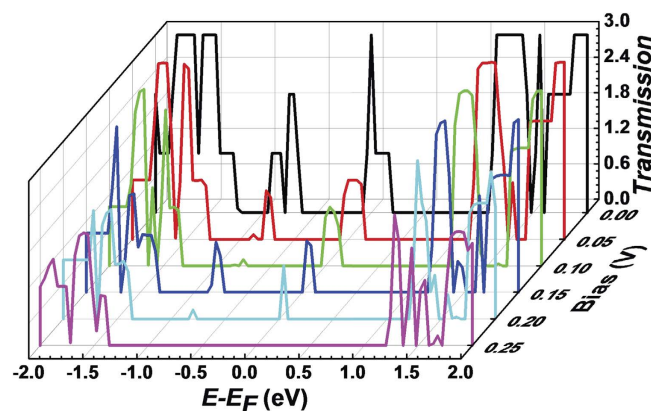


Figure 3. The transmission spectra of $W = 1.5$ zigzag C_2N - $h2D$ nanoribbon under bias $V_b = 0.00, 0.05, 0.10, 0.15, 0.20$ and 0.25 V. Zero energy is the Fermi level.

and E_D are respectively the energy values of the four subbands near the Fermi level at the Γ -point. It should also be noted that E_A is the minimum energy value of the second band above the Fermi level, E_D is the maximum value of the second band below the Fermi level, E_B is the maximum value of $n = 1$ subband and E_C is the minimum value of $n = 1'$ subband. Within the energy range of the E_{AD} , only two subbands cross each other and pass through the Fermi level. Both the left and right electrodes are semi-infinite zigzag C_2N - $h2D$ nanoribbons, so they also have such a band structure. If we apply a bias on the electrodes, an electric potential difference will appear between the two electrodes, and their band structures will shift downward or upward relatively. In the middle and right panels of Fig. 4(a), we applied a positive bias (V_+) of 0.125 V on the left electrode and a negative bias (V_-) of -0.125 V on the right electrode. As a result, there appears an energy window (the shadow region) due to the shift of the Fermi level. When the bias is low, the shadow region is small, and both $n = 1$ and $n = 1'$ subbands exist in the V_+ and V_- regions, that is to say the $n = 1$ and $n = 1'$ subbands in the V_+ region overlaps those in the V_- region. As the bias increases, the overlapping becomes smaller so that the transmission peak is getting lower. When the bias increases to 0.25 V, in the energy window, the $n = 1$ subband in the V_+ region is connected to the $n = 1'$ subband in the V_- region. Because the electrons can not hop from one subband to another, the transmission is forbidden. Interestingly, since there are sufficient gaps both in the E_{AB} and E_{CD} ranges, the tunneling channel does not exist and the insulator-like state can be maintained as the bias continues to increase. Meanwhile, we find that the insulator-like state will happen as long as E_{AB} is greater than the absolute value of E_C and E_{CD} is greater than the value of E_B . The greater E_{AB} and E_{CD} are, the greater bias range the insulator-like state can be kept in. Figure 4(b) shows the wave functions of the $n = 1$ and $n = 1'$ subbands.

In Fig. 2(a), we have pointed out that the phenomenon of NDR effect and insulator-like state also occurs in $W = 1.0$ zigzag C_2N - $h2D$ nanoribbon, whereas the same analysis is invalid for such models with an integer width. For example, the conduction should not be cut off at 0.5 V, so this abnormal phenomenon is worthy of further investigation. Figure 5(a) shows the band structure of the unit cell of the $W = 1.0$ zigzag C_2N - $h2D$ nanoribbon. It is clear that $W = 1.0$ model has the same band morphology as $W = 1.5$ model, except that the $n = 1$ and $n = 1'$ subbands are more delocalized. Figure 5(b) presents the wave functions of $n = 1$ and $n = 1'$ subbands. It is easy to see

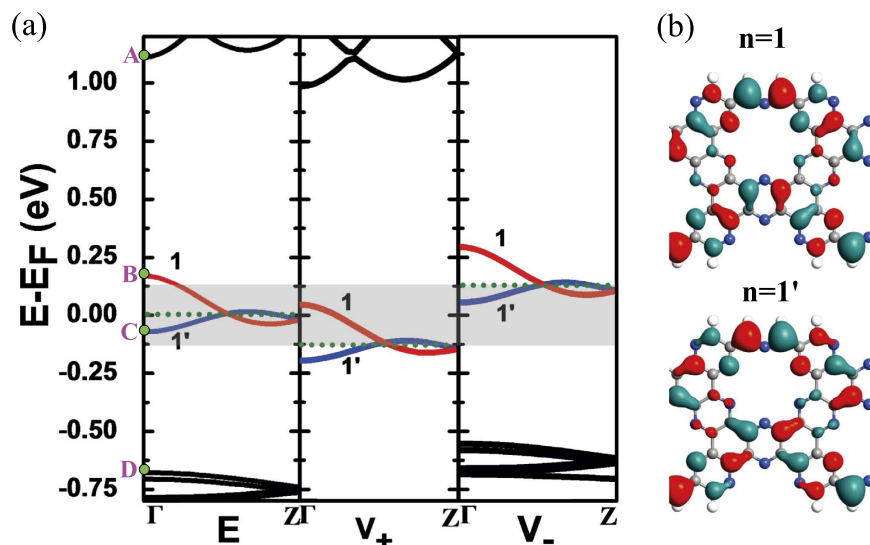


Figure 4. (a) Band structure of $W = 1.5$ zigzag C_2N - $h2D$ nanoribbon around the Fermi level. The left is without bias, the middle is under positive bias of 0.125 V and the right is under negative bias of -0.125 V. The two subbands near the Fermi level are shown in red (index $n = 1$) and blue (index $n = 1'$) respectively. The energy points of the four subbands near the Fermi level at the Γ -point are respectively represented by A, B, C and D. The dotted line is the Fermi level. (b) Isosurface plots of the Γ -point wave functions of $n = 1$ and $n = 1'$ subbands.

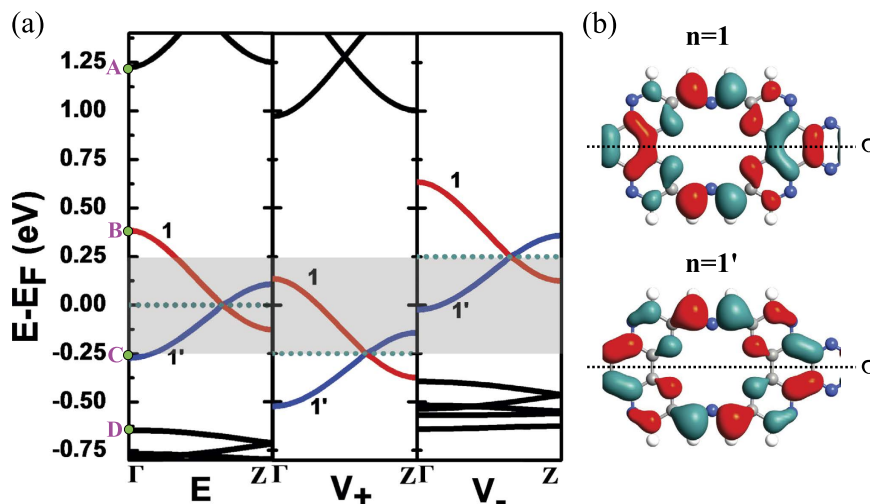


Figure 5. (a) Band structure of $W = 1.0$ zigzag C_2N - $h2D$ nanoribbon around the Fermi level. The left is without bias, the middle is under positive bias of 0.25 V and the right is under negative bias of -0.25 V. The two subbands near the Fermi level are shown in red (index $n = 1$) and blue (index $n = 1'$) respectively. The energy points of the four subbands near the Fermi level at the Γ -point are respectively represented by A, B, C and D. The dotted line is the Fermi level. (b) Isosurface plots of the Γ -point wave functions of $n = 1$ and $n = 1'$ subbands.

that the $n = 1$ subband has even parity, nevertheless, the $n = 1'$ subband has odd parity under σ mirror operation. Since these two subbands have opposite σ parity, an electron belonging to $n = 1'$ subband (blue) can not hop to $n = 1$ (red) subband^{18,19}, so the subbands with different colors can not couple with each other. Simultaneously, we should note that the $n = 1$ and $n = 1'$ subbands have no parity for $W = 1.5$ model due to its asymmetric structure as shown in Fig. 4(b), so the electrons can hop between them. This phenomenon has been reported in graphene and its related structures¹⁹. Under a low bias, there exists an overlapping between the subbands in the V_+ and V_- region, but the electron transport only comes from the coupling between the same color subbands. When the bias increases to 0.5 V, the $n = 1$ subbands in the V_+ and V_- region are connected in the energy window. However the $n = 1$ subband in the V_+ region and the $n = 1'$ subband in the V_- region have different parity, and the tunneling between these two subbands is forbidden, so that the current is reduced to zero. This state is held as the bias continues to increase. When the bias is high, we can find the insulator-like state is still derived from the presence

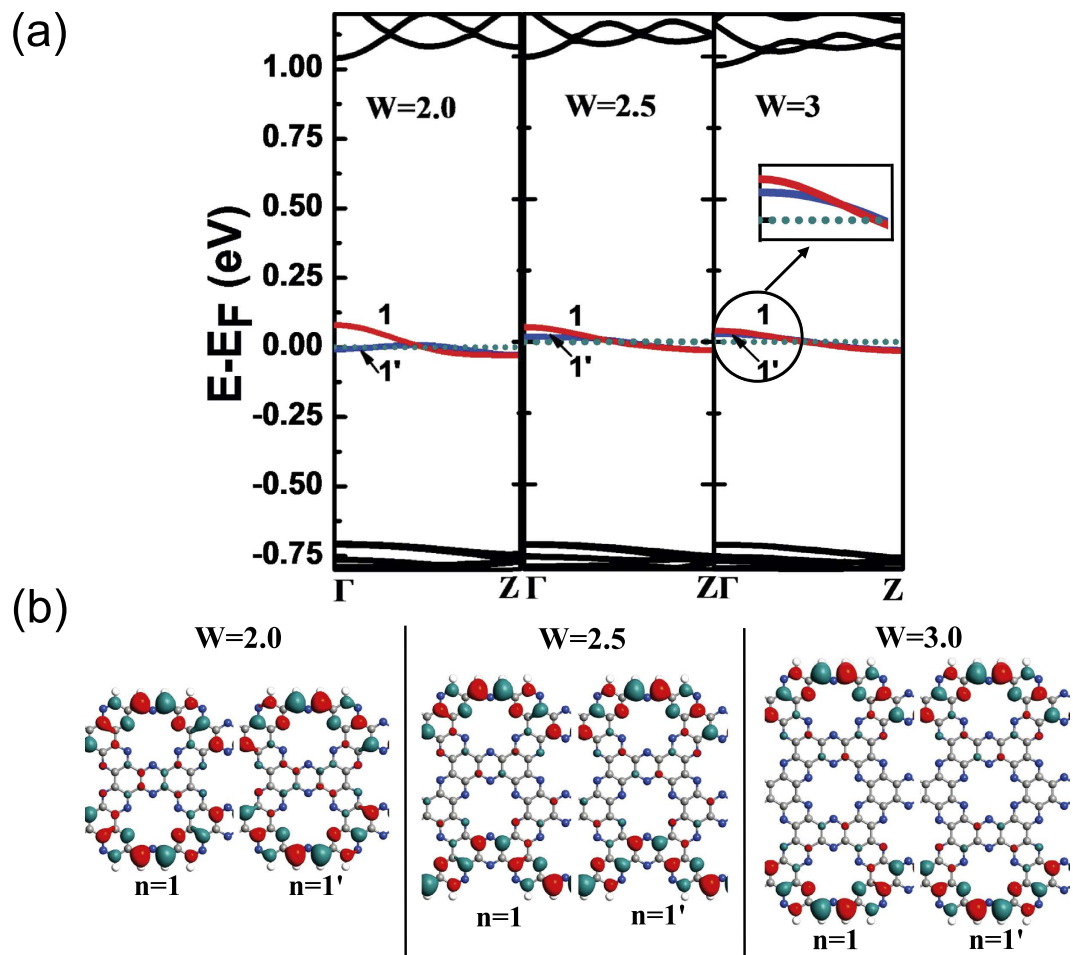


Figure 6. (a) Band structures of zigzag C_2N - $h2D$ nanoribbon around the Fermi level with different widths ($W = 2.0, 2.5$ and 3.0). The two subbands nearest to the Fermi level are shown in red (index $n = 1$) and blue (index $n = 1'$) respectively. The dotted line is the Fermi level. (b) Isosurface plots of the Γ -point wave functions of $n = 1$ and $n = 1'$ subbands.

of band gaps in the range of E_{AB} and E_{CD} . Consequently, the phenomena of NDR effect and insulator-like state of $W = 1.0$ model originate from the peculiar band morphology too, except that the different parity between the subbands near the Fermi level prevents the electron transport and promotes the insulation-like state to happen in lower bias.

To explore the effect of width on the electron property of zigzag C_2N - $h2D$ nanoribbon, we calculated the band structures of other models with different widths shown in Fig. 6(a). It can be seen that $W = 2.0, 2.5$ and 3.0 models have the same band morphology as $W = 1.0$ and 1.5 models, so the width does not change the main characteristics of band structure. However, as the width increases, the $n = 1$ and $n = 1'$ subbands become more localized. In Fig. 6(b), we present the wave functions of $n = 1$ and $n = 1'$ subbands. Obviously, for wider structures, the wave functions are more localized on the edge indicating the $n = 1$ and $n = 1'$ subbands are edge states which look very similar to those in zigzag graphene nanoribbons^{20,21}. However, there is a little difference between them. In zigzag graphene nanoribbons, the localized edge states form a degenerate flat band at the Fermi level, but for our models, the subbands near the Fermi level are non-degenerated which may be caused by the introduction of N atoms²². And for $W = 2.0$ and $W = 3.0$ structures, the $n = 1$ subband has even parity and the $n = 1'$ subband has odd parity which is the same as $W = 1.0$ model. For $W = 2.5$ structure, $n = 1$ and $n = 1'$ subbands have no parity due to the asymmetric nanoribbon. We can conclude that as the width increases the NDR effect and the insulator-like state still exist, but the cut-off bias will become smaller due to the more localized subbands. These properties offer an interesting method by modifying the width of the zigzag C_2N - $h2D$ nanoribbon to tune the cut-off bias in future applications.

In the above analysis, we focus on the investigation of theoretical physical mechanism. Taking into account the possibility of experimental operation and practical application, a finite bias voltage could not be applied in a homogeneous situation with discrete translational symmetry, in order to avoid this problem we design the device of W2-1 as shown in Fig. 7(a). The central scattering region is formed by the combination of $W = 2.0$ and $W = 1.0$ nanoribbons. After optimization, some atoms at the interface of the scattering region are disturbed. To explore the influence of disturbing part on the electronic transport properties, we construct another structure W2-1-H

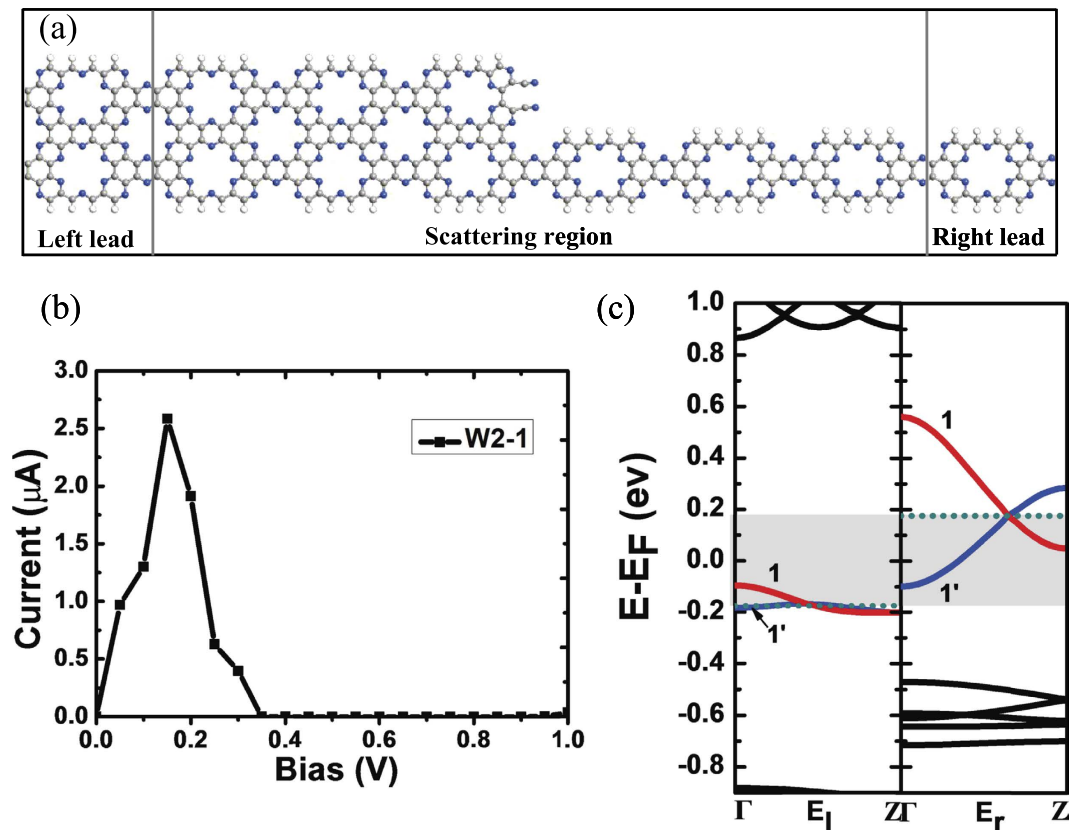


Figure 7. (a) Schematic illustration of the W2-1 model. Nitrogen, carbon and hydrogen atoms are shown by blue, gray and white balls, respectively. (b) The current-voltage curve of W2-1 model in the bias range from 0.0 to 1.0 V. (c) Band structures of the left electrode (E_l) and right electrode (E_r) of W2-1 model around the Fermi level under bias of 0.175 V and -0.175 V respectively. The two subbands nearest to the Fermi level are shown in red (index $n = 1$) and blue (index $n = 1'$) respectively. The dotted line is the Fermi level.

(not shown here), two carbon atoms which were separately terminated by nitrogen atoms at the center of the scattering region are passivated by H atoms and the carbon ring has not been opened. The W2-1-H model maintains the same transport characteristics as W2-1 device. Therefore, it can be concluded that the disturbance has little effect on the whole transport properties. Figure 7(b) presents the current-voltage (I - V) characteristic of the device W2-1. It can be seen that the morphology of the I - V curve is similar to that of $W = 1.0$ model which is shown in Fig. 2(a). There appears an obvious negative differential resistance phenomenon. The current firstly increases as the bias increases, then begins to reduce at the bias of 0.15 V, and finally reduces to zero while the bias is 0.35 V. This insulator-like state can be maintained until the bias increases to 1.0 V. We also calculate the potential drop of the W2-1 device (not shown here), and find the potential drop mainly occurs at the center of the scattering region, so the electron scattering mainly happens around this region. In order to inspect the physics mechanism behind the phenomenon of negative differential resistance and the insulator-like state, similar to previous analysis, we calculate the band structures of the left and right electrodes of the device W2-1 in Fig. 7(c).

It can be seen that when we apply a positive bias on the device, the band structures of the left and right electrodes will shift downward or upward relatively. If the bias is low, the shadow region becomes smaller, and there will be both $n = 1$ and $n = 1'$ subbands in the E_l and E_r regions. The electrons can hop between them, so the current firstly increases. When the bias is larger than 0.15 V, $n = 1$ subbands do not overlap leaving only the $n = 1'$ subbands to contribute to the transmission, so the current starts to decrease. When the bias increases to 0.35 V, as show in Fig. 7(c), the $n = 1'$ subband in the E_l region is slightly far away from the $n = 1'$ subband in the E_r region. According to our previous analysis, the current should be zero when these two $n = 1'$ subbands are connected under a bias less than 0.35 V. It is noteworthy that some disturbance appears in the center of the scattering region after optimization, so the energy levels of the central part are a little different from the electrodes. That is why the current becomes zero at a higher bias. When the bias continues to increase, the current can be maintained at zero. This insulator-like state still derives from the peculiar band morphology which possesses a sufficient band gap between these two $n = 1'$ subbands. The physics mechanism is consistent with what we discussed previously.

Discussion

In our research, we find that this mechanism can be extended to other systems, that is to say, as long as the structure has the similar band morphology, this phenomenon that the current in NDR effect can be reduced to zero and the insulator-like can be maintained will happen. For example, Kan *et al.*²³ have reported that half-metallicity can

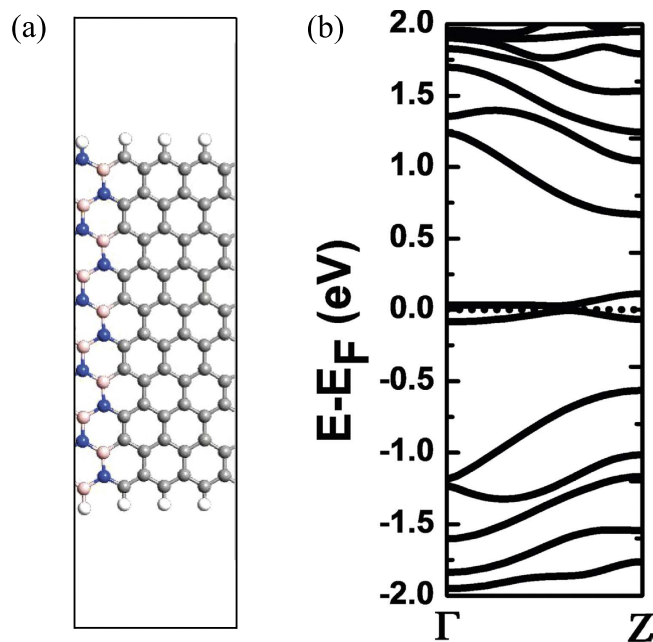


Figure 8. (a) The unit cell of C and BN hybrid zigzag nanoribbon. Nitrogen, boron, carbon and hydrogen atoms are shown by blue, pink, gray and white balls, respectively. (b) Band structures of C and BN hybrid zigzag nanoribbon around the Fermi level. The dotted line is the Fermi level.

arise in hybrid BCN nanoribbons. In Fig. 8, we give out the unit cell of the C and BN hybrid zigzag nanoribbon and its band structure. Obviously, there are only two subbands near the Fermi level, while others are far away. So it can be predicted that this phenomenon will occur in the hybrid BCN structure. Due to the limitation of the computational conditions, we do not give out the I - V curve here.

In summary, the electronic and transport properties of the zigzag C_2N - $h2D$ nanoribbons with different widths are studied using first-principles calculations. By cutting into nanoribbon, C_2N - $h2D$ changes from the original semiconductor to metallic structure owing to the introduced two edge states near the Fermi level. The band morphologies for all the nanoribbons have the same special characteristic, i.e., there are only two subbands near the Fermi level while other subbands are far away which leads to the emergence of gaps. To explore the physical mechanism, we give some homogeneous models. An obvious NDR effect and an insulator-like state occur in the I - V curve which has not been reported in such a nano-sized periodic structure in previous works. For asymmetric structures ($W = 1.5$ and 2.5), this phenomenon originates from the peculiar band morphology. For symmetric structures ($W = 1.0, 2.0$ and 3.0), besides the peculiar band morphology, the opposite parity of the two edge states is also a factor as it prevents some electron transport and promotes the insulation-like state to happen in lower bias. In addition, as the width increases, the two edge states become more localized, and the cut-off bias decreases. Therefore we can tune the electron transport by changing the width of the zigzag C_2N - $h2D$ nanoribbon. We also show a heterogeneous model composed of two zigzag C_2N - $h2D$ nanoribbons with different widths. It has a similar I - V curve, the peculiar band morphology still plays a decisive role and the disturbance in the center of the scattering region leads to the occurrence of the insulator-like in a little higher bias. We can also predict that for other materials, as long as they have similar band morphologies, the NDR and insulation-like state will happen.

Methods

To investigate the transport property of our system accurately, the Atomistix Toolkit (ATK) package which is based on the combination of density functional theory (DFT) and non-equilibrium Green's function (NEGF) technique is performed²⁴. The mesh cutoff energy is set to 150 Ry, and the k -point mesh is $1 \times 1 \times 100^{25}$. The Perdew-Burke-Eenzerhof formulation of the generalized gradient approximation (GGA) is used as the exchange-correlation function, and the double-zeta polarized basis set is employed in the calculations. The vacuum spaces of supercell are set to be more than 15 \AA to prevent the interaction with adjacent images. All the atomic positions of the structure have been optimized until all the forces are smaller than 0.01 eV/\AA . The edges of zigzag C_2N - $h2D$ nanoribbon are terminated with hydrogen (H) atoms to remove the dangling bonds.

In NEGF theory, the current of the two-probe system is calculated based on the Landauer-Büttiker formula

$$I(V) = \frac{2e}{h} \int T(E, V) [f(E - \mu_L) - f(E - \mu_R)] dE, \quad (1)$$

where $\mu_{L(R)}$ is the chemical potential of the left (right) electrode, $f(E - \mu_{L(R)})$ is the Fermi distribution of the left (right) electrode, and $V = (\mu_L - \mu_R)/e$ represents the bias window. $T(E, V)$ is the transmission coefficient obtained by using Green's function. Clearly, the current is determined by the area of the integral region in the bias window.

References

1. Avouris, P. & Chen, Z. H. Perebeinos & Vasili Carbon-based electronics. *Nat. Nanotech.* **2**, 605–615 (2007).
2. Geim, A. K. & Novoselov, K. S. The rise of graphene. *Nat. Mater.* **6**, 183–191 (2007).
3. Deretzis, I., Fiori, G., Iannaccone, G. & La Magna, A. Effects due to backscattering and pseudogap features in graphene nanoribbons with single vacancies. *Phys. Rev. B* **81**, 085427 (2010).
4. Zhang, R. Q., Li, B. & Yang, J. L. Effects of stacking order, layer number and external electric field on electronic structures of few-layer C_2N - h_2D crystals. *Nanoscale* **7**, 14062–14070 (2015).
5. Schwierz, F. Graphene transistors. *Nat. Nanotech.* **5**, 487–496 (2010).
6. Liao, L. *et al.* High-speed graphene transistors with a self-aligned nanowire gate. *Nature* **467**, 305–308 (2010).
7. Novoselov, K. S. *et al.* Two-dimensional gas of massless Dirac fermions in graphene. *Nature* **438**, 197–200 (2005).
8. Mahmood, J. *et al.* Nitrogenated holey two-dimensional structures. *Nat. Commun.* **6**, 6486 (2015).
9. Sahin, H. Structural and phononic characteristics of nitrogenated holey graphene. *Phys. Rev. B* **92**, 085421 (2015).
10. Esaki, L. New phenomenon in narrow germanium p-n junctions. *Phys. Rev.* **109**, 603 (1958).
11. Mizuta, H. & Tanoue, T. The Physics and Applications of Resonant Tunneling Diodes. *J. Phys. Soc. Jpn* **51**, 444 (1995).
12. Zhang, X. J. *et al.* Electronic transport properties in doped C60 molecular devices. *Appl. Phys. Lett.* **94**, 73503 (2009).
13. Fan, Z. Q. *et al.* Theoretical investigation of the negative differential resistance in squashed C60 molecular device. *Appl. Phys. Lett.* **92**, 263304–263304 (2008).
14. Ren, H., Li, Q. X., Luo, Y. & Yang, J. L. Graphene nanoribbon as a negative differential resistance device. *Appl. Phys. Lett.* **94**, 173110 (2009).
15. Do, V. & Dollfus, P. Negative differential resistance in zigzag-edge graphene nanoribbon junctions. *J. Appl. Phys.* **107**, 063705 (2010).
16. Khoo, K. H., Neaton, J. B., Son, Y. W., Cohen, M. L. & Louie, S. G. Negative differential resistance in carbon atomic wire-carbon nanotube junctions. *Nano Lett.* **8**, 2900–2905 (2008).
17. Li, X. F., Wang, L. L., Chen, K. Q. & Luo, Y. Electronic transport through zigzag/armchair graphene nanoribbon heterojunctions. *J. Phys.: Condens. Matter* **24**, 095801 (2012).
18. Wang, Z. F. *et al.* Chiral selective tunneling induced negative differential resistance in zigzag graphene nanoribbon: A theoretical study. *Appl. Phys. Lett.* **92**, 133114 (2008).
19. Li, Z. Y., Qian, H. Y., Wu, J., Gu, B. L. & Duan, W. H. Role of symmetry in the transport properties of graphene nanoribbons under bias. *Phys. Rev. Lett.* **100**, 206802 (2008).
20. Fujita, M., Wakabayashi, K., Nakada, K. & Kusakabe, K. Peculiar localized state at zigzag graphite edge. *J. Phys. Soc. Jpn.* **65**, 1920–1923 (1996).
21. Nakada, K., Fujita, M., Dresselhaus, G. & Dresselhaus, M. Edge state in graphene ribbons: Nanometer size effect and edge shape dependence. *Phys. Rev. B* **54**, 17954 (1996).
22. Son, Y. W., Cohen, M. & Louie, S. Half-metallic graphene nanoribbons. *Nature* **444**, 347–349 (2006).
23. Kan, E. J. *et al.* Half-metallicity in hybrid BCN nanoribbons. *J. Chem. Phys.* **129**, 084712 (2008).
24. Brandbyge, M., Mozos, J. L., Ordejon, P., Taylor, J. & Stokbro, K. Density-functional method for nonequilibrium electron transport. *Phys. Rev. B* **65**, 165401 (2002).
25. Monkhorst, H. & Pack, J. Special points for Brillouin-zone integrations. *Phys. Rev. B* **13**, 5188 (1976).

Acknowledgements

Thanks to Dr. Wei Zhao for his helpful discussion. This work is supported by the National Natural Science Foundation of China (NSFC11504178, NSFC11374162, NSFC11247033 and NSFC51651202), the Natural Science Foundation of Jiangsu Province (BK20150825 and TJ215009), the Scientific Research Foundation of Nanjing University of Posts and Telecommunications (NY214010), and the Fundamental Research Funds for the Central Universities (NS2014073).

Author Contributions

J.H. contributed the idea, the calculations and the preparation of the manuscript. Y.G. contributed the analysis of the results. X.Y. supervised the whole project.

Additional Information

Competing Interests: The authors declare no competing financial interests.

How to cite this article: He, J.-J. *et al.* Negative differential resistance and bias-modulated metal-to-insulator transition in zigzag C_2N - h_2D nanoribbon. *Sci. Rep.* **7**, 43922; doi: 10.1038/srep43922 (2017).

Publisher's note: Springer Nature remains neutral with regard to jurisdictional claims in published maps and institutional affiliations.



This work is licensed under a Creative Commons Attribution 4.0 International License. The images or other third party material in this article are included in the article's Creative Commons license, unless indicated otherwise in the credit line; if the material is not included under the Creative Commons license, users will need to obtain permission from the license holder to reproduce the material. To view a copy of this license, visit <http://creativecommons.org/licenses/by/4.0/>

© The Author(s) 2017